Kingdom Saudi Arabia

Al-Imam Muhammad
Saud Islamic University
College of Department
of Chemistry

المملكة العربية السعودية

جامعة الإمام محمد بن سعود الإسلامية

كلية العلوم

قسم الكيمياء

Preparation, Characterization and Application of Nanosized Copper Ferrite Photocatalyst for Dye Degradation

A graduation research project submitted to the Department of Chemistry in partial fulfillment of the requirement for the completion of a degree of science in chemistry

By

Anwar Aftan AlDhahi, ID: 440028553

Fay Shaya Alqahtani, ID: 441018274

Lina Hajjaj Alhajjaj, ID: 441018810

Hala Mubarak Almouh, ID: 440027199

Haifa Mohammed Bin Owais, ID: 441020300

Under supervision of

Dr. Nuha Yousif

Second Semester, February. 2024

Table of Content:

Table of Figures:

Abstract:

In this study copper Ferrite nanoparticles were synthesized using Foeniculum vulgare seeds extract. The obtained copper Ferrite nanoparticles were characterized by SEM, EDX, FTIR, XRD and BET (surface area) techniques. SEM images for surface morphology of $CuFe_2O_4$ nanocomposites observed that there are spherical shaped particles with different sizes. with diameter in the range from 30.8-43.6 nm. The results of EDX analysis showed the presence of iron (Fe), copper (Cu), and oxygen (O) elements in the $CuFe_2O_4$ nanocomposites with weight percent equal to 40.3%, 27.0% and 32.7% respectively. FT-IR spectrum showed a broadband at 3440 cm-1 indicates that there is moisture on the surface of $CuFe_2O_4$ nanocomposite. The absorption at 415 .55 cm^{-1} is related to the stretching vibration of Cu-O, and the appearing absorption at 579.02 and 589.77 cm-1 is related to the stretching vibration of Fe-O. The XRD pattern shows that the synthesized $CuFe_2O_4$ NPs were polycrystalline in nature. The pore size distribution and N_2 adsorption –desorption isotherm was confirmed by BET analysis of copper ferrite nanoparticles. The results indicate that $CuFe_2O_4$ NPs have a surface area of 20.35m^2/g, and pore volume and pore size corresponding to 0.092cm^3/g and 161.230 Å, respectively. The adsorption and photocatalytic capacities of the $CuFe_2O_4$ were examined for the malachite green dye (MG) as a model water-pollutant via the batch experiment methodology. The solution parameters were optimized, including contact time and MG concentration. Worth mentioning that an adsorption capacity of 17.71 $mg \cdot g^{-1}$ was obtained from 100 mg L^{-1} MG solution at 25 °C within 240 min as an equilibrium time. The Optimum pH was at 8 with adsorption of 69.76%. In addition, the $CuFe_2O_4$ showed a high degradation efficiency towards MG under tungsten lamp (80 W), where 99% was removed. The fabricated $CuFe_2O_4$ nanoparticles completely mineralized the MG under artificial visible light.

الخلاصة:

في هذه الدراسة، تم تصنيع جسيمات النحاس المغناطيسية النانوية باستخدام مستخلص بذور الشمر تم تشخيص الجسيمات النانوية المغناطيسية المصنوعة من النحاس بتقنيات حيود الأشعة السينية، المسح المجهري الإلكتروني مع تحليل الأشعة السينية المشتتة للضوء والتحليل الطيفي للأشعة تحت الحمراء و محلل امتصاص النيتروجين للمواد المسامية. كشفت صور المسح المجهري الإلكتروني عن جسيمات كروية الشكل بأحجام مختلفة تتراوح أقطارها بين 30.8 و 43.6 نانومتر ، كما أظهرت نتائج تحليل الأشعة السينية المشتتة للضوء وجود عنصر الحديد ، النحاس والأكسجين في جسيمات النحاس المغناطيسية النانوية بنسب مئوية تبلغ 40.3٪ و 27.0٪ و 32.7٪ ، أظهرت أطياف الأشعة تحت الحمراء نطاقًا عريضًا عند 3440 سم $^{-1}$ يوضح وجود رطوبة على سطح جسيمات النانو ، يرتبط الامتصاص عند 415.55 سم $^{-1}$ بالاهتزاز التمددي للنحاس- أكسجين، بينما يرتبط الامتصاص عند 579.02 و 589.77 سم$^{-1}$ بالاهتزاز التمددي للحديد – أكسجين. وأظهر نمط حيود الأشعة السينية أن جسيمات النانو هي بالفعل جسيمات النحاس المغناطيسية. تم تأكيد توزيع حجم المسام و امتصاص-امتزاز النيتروجين خط متساوي الحرارة من خلال تحليل تحليل مساحة السطح للمواد المسامية للجسيمات النحاس المغناطيسية. تشير النتائج إلى أن جسيمات النانو لها مساحة سطح تبلغ 20.35 م 2 / جرام، حجم مسام وسعة مسام يبلغ 0.092 سم ^{3} / جرام و 161.230 انجستروم على التوالي. تم اختبار قدرة الامتصاص والتحفيز الضوئي لجسيمات النانو على صبغة الملاكيت الخضراء كنموذج لمادة تلوث المياه باستخدام منهجية تجربة الدفعة. تم تحسين معلمات المحلول، بما في ذلك وقت التلامس وتركيز صبغة الملاكيت الخضراء تبلغ قدرة الامتصاص 17.71 ملجم · جرام $^{-1}$ التي تم الحصول عليها من محلول صبغة الملاكيت الخضراء عند 25 درجة مئوية خلال 240 دقيقة كوقت توازن ، كان الرقم الهيدروجيني الأمثل عند 8 مع امتصاص بنسبة 69.76%. بالإضافة إلى ذلك أظهرت جسيمات النانو كفاءة تحليل عالية تجاه صبغة الملاكيت الخضراء تحت مصباح التنغستن (80 واط)، حيث تمت إزالة 99٪. قامت جسيمات النانو النحاسية المغناطيسية المصنعة بتحويل صبغة الملاكيت الخضراء بالكامل تحت الضوء المرئي الاصطناعي.

Chapter 1

Introduction and Literature Review

1.1 Nanotechnology:

Nanotechnology can be defined as the science and engineering involved in the design, synthesis, characterization, and application of materials and devices whose smallest functional organization in at least one dimension is on the nanometer scale or one billionth of a meter. At these scales, consideration of individual molecules and interacting groups of molecules in relation to the bulk macroscopic properties of the material or device becomes important, since it is control over the fundamental molecular structure that allows control over the macroscopic chemical and physical properties [1]. The science of atoms and simple molecules and the science of matter from micro-structures to larger scales are generally established, in parallel. The remaining size related challenge is at the nanoscale where the fundamental properties of materials are determined and can be engineered. A revolution has been occurring - ring in science and technology, based on the ability to measure, manipulate, and organize matter on this scale. These properties are incorporated into useful and functional devices. Therefore, nanoscience will be transformed into nanotechnology [2]

1.2 Nanomaterial:

Nanometer-scaled materials could be defined as specimens that have at least one dimension of less than 100 nm. Nanomaterials include ultrathin films, quantum wire, and nanoparticles-quantum dots, in general. Those remarkable features may include special optical, magnetic, and electrical properties, among many others. These unique properties could potentially have great impacts on electronics, spintronics, medical applications, and other devices. There are two main reasons why nanomaterials have properties that are different from corresponding bulks: a large surface area and confinement (quantum) effects. Due to their structures that contain many small grains, nanomaterials have a much greater surface area to volume ratio than their conventional counterparts, leading to a possibility of having greater chemical reactivity; this may affect pressure inside the lattice. Moreover, at the nanometer scale, confinement effects should play a key role in shaping the properties and characteristics of materials. As a result, new optical, electrical, and magnetic behaviors may occur [3]

1.3 Synthesis of Nanomaterial:

Formation of nanosized materials - nanoparticles, nano- porous or nanostructured macroscopic materials – is achieved by two basic routes, namely the so-called top-down and bottom-up methods. In the former, macroscopic materials are used to

fabricate nanomaterial and nanostructures using - typically - very sophisticated methods. In the latter, nanoparticles and other nanomaterials are built up from their ultimate building blocks - atoms and molecules - via self-assembly processes. In the top-down method we start from bulk materials and fabricate structures or particles on the nanoscale, analogously to the carving of a sculpture (or many small ones) from a mar [4].

1.3.1 Top-down

The top-down method is a destructive method of nanoparticle synthesis. It is based on the decrement of bulk materials into nanometric-scale materials. Mechanical ball milling. thermal decomposition, and laser ablation are the most widely used top-down methods for nanomaterial synthesis. mechanical grinding is a common example of top-down approach [5]

1.3.2 Bottom-up

The principle of the bottom-up approach is based on the building up of nanoparticles from atomic level through the formation of clusters. colloidal dispersion is a typical example of bottom-up approach [6].

1.4 Classification of Nanomaterials

A nanostructure can be described and classified on the basis of the number of dimensions that belong to the nanoscale [6]

1.4.1 One-dimensional nanostructures (1D)

These types of nanoparticles are at least one dimension larger than nanoscales and other dimensions are within the nano range. The most common examples of one-dimensional nanoparticles are nanofibers, nanotubes, and nanorods [7].

1.4.2 Two-dimensional complex materials (2D)

2D nanomaterials should be the thinnest nanomaterials due to their low thickness and higher dimensions on macroscale/nanoscale. These nanomaterials possess generally a layered structure with strong in-plane bonds and weak interaction forces (van der Waals) within the layers and can be produced by laminating precursors. The matter of the fact is that, since two of the dimensions are not confined to the nanoscale, 2D nanomaterials show plate-like shapes, such as nanofilms, nanolayers, and nanocoating's, and can be amorphous or crystalline, of various chemical compositions, applied as a single layer or as multilayer structures, used placed on a substrate, be integrated into a complex matrix of materials, and of course be metallic, ceramic, or

polymeric. Graphene, hexagonal boron nitride (hBN), and metal dichalcogenides (MX2) are examples of this category [8].

1.4.3 Three-dimensional nanostructures (3D)

There are also bulk materials with all dimensions above 100 nm and are named three-dimensional nanostructures (3D). Materials having a nanocrystalline structure or involving the presence of features at the nanoscale are examples of this dimensionality. 3D nanomaterials can be composed of dispersions of nanoparticles, bundles of nanowires, and nanotubes as well as multinanolayers, but more complex arrangements are possible. Nanoflowers are for instance a kind of possible architecture [8].

1.5 Preparation of Nanoparticles

The preparation of nanoparticles is a critical part of obtaining the desired size, shape, composition, and functionality of the particles. There are different methods for preparing nanoparticles, choosing the best method depends on the requirements of the specific application. These methods can be classified into two main categories: chemical and physical methods. Chemical methods involve using chemical reactions to produce nanoparticles from different precursors in solvents. Physical methods involve using physical impact or energy to break down bulk materials into nanoparticles. Some of the most important methods of nanoparticle preparation will be reviewed in the following section, each method has its own advantages and disadvantages, such as cost, purity, stability, and control over particle size and shape. [9, 10]

1.5.1 Co-Precipitation Method

The coprecipitation technique is becoming increasingly important to distribute materials and precursors used in a reaction to produce a required material. The precursor material of the nanoparticles was chemically precipitated by mixed aqueous solutions of metallic salts. The aim of coprecipitation is to prepare multicomponent materials through the formation of intermediate precipitates, usually hydrous oxides or oxalates so that an intimate mixture of components is formed during precipitation and chemical homogeneity is maintained on calcination. [11, 12]

In the typical process of co-precipitation, aqueous metal salts are mixed at sufficient temperatures with a base, which acts as a precipitating agent. This method is widely employed for synthesis. However, in a few cases, the process is performed under an inert atmosphere. The advantage of the coprecipitation method is that it gives a

crystalline size in a small range compared to other synthesis processes depending on the precipitating agent selected during the reaction. [12]

1.5.2 Sol-Gel Method

The Sol-gel method is the simplest method and has the ability to control the particle size and morphology through systematic monitoring of reaction parameters. The sol-gel method has many advantages, such as product purity and, among the most important ones, the possibility to incorporate thermolabile molecules. In fact, it is possible to obtain organic—inorganic hybrid materials, in which the organic and inorganic phase are bonded together at the nanometer to sub-micrometer scales. [13, 14]

The starting point for synthesizing sol—gel materials is to understand the chemistry behind this method. In the synthesis process, molecular precursors, such as metal alkoxides, are used, which are involved in two important reactions: hydrolysis and polycondensation. The drying stage is a critical part of the whole sol—gel process, which involves the removal of the liquid phase from the wet gel. As evaporation occurs, drying stress can cause the cracking of bulk materials. During the drying process, the gel shrinks by the volume that was previously occupied by the liquid, which flows from the internal of the gel body to its surface. [14]

The sol—gel process is preferred due to its economic feasibility and that the low-temperature process allows control over the composition of the product that is achieved. Most of the materials prepared by the sol—gel method are advanced materials needed for the development of advanced technologies. [14, 15, 16, 17]

1.5.3 Hydrothermal Method

Hydrothermal synthesis refers to the synthesis by chemical reactions of substances in a sealed heated solution above the ambient temperature and pressure. Hydrothermal synthesis of single crystals depends on the solubility of minerals in hot water under high pressure. The crystal growth is performed in an apparatus consisting of a steel pressure vessel called an autoclave, in which a nutrient is supplied along with water. A gradient of temperature is maintained at the opposite ends of the growth chamber so that the hotter end dissolves the nutrient and the cooler end causes seeds to take additional growth. The hydrothermal synthesis has been successful in the preparation of important solids, such as microporous crystals, superionic conductors, chemical sensing oxides, electronically conducting solids, complex oxide ceramic and fluorides, magnetic materials, and luminescence phosphors. It is also a route to unique condensed

material, including nanometer particles, gels, thin films, distinguished helical and chiral structures, and particularly stacking-sequence materials. [17]

1.5.4 Microwave Method

The microwave method is a physical approach for the synthesis of nanoparticles that uses microwave radiation to heat the reaction medium and induce nucleation and growth of nanoparticles. The microwave method has several advantages over conventional heating methods, such as rapid and uniform heating, high energy efficiency, easy control, and scalability. Some of the factors that affect the microwave synthesis of nanoparticles are microwave power, irradiation time, precursor concentration, solvent type, and stabilizing agent.[18]

Microwave-assisted synthesis is popular in areas ranging from biochemical processes to nanotechnology. Chemical reactions are often faster than traditional convection heating methods and have high yields and fewer side products. Microwave reactors provide excellent control over reaction mixing, withstanding high temperatures and pressures, and demonstrate reproducibility from reaction to reaction. Microwave assisted techniques provide improved engineering control over the separation of the nucleation and growth stages of nanomaterial synthesis when the reaction is initiated from room temperature. Microwave-assisted heating could possibly provide some selectivity in activating the nanomaterial precursor materials, which is important for scalability. Microwave synthesis has the potential to selectively heat either the solvent or the precursor molecules for nanomaterial preparation. [17]

1.6 Characterization of Nanoparticles

Many techniques can be employed for nanoparticle/nanomaterial characterization. Are scanning electron microscopic (SEM), surface area brunauer Emmett Teller (BET), X-Ray diffraction analysis, Fourier transform infrared spectroscopy (FT-IR) and Energy dispersive X-Ray (EDX). [19]

1.6.1 scanning electron microscopic (SEM)

Scanning electron microscopy (SEM) is giving morphological examination with direct visualization. The techniques based on electron microscopy offer several advantages in morphological and sizing analysis; however, they provide limited information about the size distribution and true population average. For SEM characterization, nanoparticles solution should be first converted into a dry powder, which is then mounted on a sample holder followed by coating with a conductive metal, such as gold, using a sputter coater.

The sample is then scanned with a focused fine beam of electrons. The surface characteristics of the sample are obtained from the secondary electrons emitted from the sample surface. The nanoparticles must be able to withstand vacuum, and the electron beam can damage the polymer. The mean size obtained by SEM is comparable with results obtained by dynamic light scattering. Moreover, these techniques are time consuming, costly and frequently need complementary information about sizing distribution (Molpeceres et al., 2000).[20]

1.6.2 Surface are Brunauer-Emmett-Teller (BET)

The Langmuir theory has a few flaws that are addressed by the BET theory. The BET theory extends the Langmuir theory to multilayer adsorption with three additional assumptions: • Gas molecules will physically adsorb on a solid in layers infinitely. • The different adsorption layers do not interact. • The theory can be applied to each layer. Adsorption is defined as the adhesion of atoms or molecules of gas to a surface. The amount of gas adsorbed depends on the exposed surface are but also on the temperature, gas pressure and strength of interaction between the gas and solid. In BET surface area analysis, nitrogen is usually used because of its availability in high purity and its strong interaction with most solids. The BET technique has some disadvantages when compared to NMR, which can also be used to measure the surface area of nanoparticles. BET measurements can only be used to determine the surface area of dry powders. This technique requires a lot of time for the adsorption of gas molecules to occur. A lot of manual preparation is required. [21]

1.6.3 X-Ray diffraction analysis (XRD)

Powder X-ray diffraction (XRD) is a common characterization technique for nanoscale materials. Analysis of a sample by powder XRD provides important information that is complementary to various microscopic and spectroscopic methods. Powder XRD provides useful information about structure, phase, composition, shape, size, crystallinity, and other important features of nanoscale materials, although unambiguous sample characterization almost always requires complementary experimental and/or computational methods. Powder XRD data for nanoscale materials can often be straightforward to analyse for the key information that is needed, but other times, it can be quite complex. [22]

1.6.4 Fourier transform infrared spectroscopy (FT-IR)

FTIR is used for detecting the functional groups in a chemical compound, the same principle is used for analysing nanomaterials. This is particularly useful in cases such as surface-modified nanomaterials for increasing their affinity, reactivity, or compatibility. Analysing a nanomaterial using FTIR tells us which functional groups are present and then the appropriate surface-modification strategy can be decided based on the groups present. Further, it can also be useful in characterizing the surface modification that has been carried out, as new groups should emerge if the reaction is successful. [23]

1.6.5 Energy dispersive X-ray (EDX)

X-ray microanalysis (EDS) provides a method to identify elements within thin and thick specimens with high sensitivity and precise location, particularly with thin specimens examined with a field-emission gun-equipped TEM. Electrons are arranged in a series of shells (K, L, M, etc.) around an atom's nucleus, with the shells nearest the nucleus having the least energy. If an electron is removed from the shell of an atom by an elastic collision of an electron from the primary beam, an ion is produced. To stabilize the ion, an electron from a higher-energy orbit (outer shell) must fill the gap fund when the electron is ejected from the atom. An amount of energy equal to the difference in energy between the outer shell and the inner shell is released in the form of an auger electron, a photon of light, or an X-ray photon. The X-ray energy is the potential energy difference between the two shells. [24]

1.7 Magnetic Nanoparticles:

Magnetic nanoparticles are a class of nanoparticle that can be manipulated using magnetic fields. Such particles commonly consist of two components, namely a magnetic material, often iron, nickel, and cobalt, and a chemical component that has functionality, frequently with (bio)catalytic or bio recognition properties. Magnetic nanoparticles, magnetic nano-rods, and other magnetic nano-species have been prepared, and used in many important applications. Particularly, magnetic nano-species functionalities with bimolecular and catalytic entities have been synthesized and extensively used for many biocatalytic, (bio)analytical, and biomedical applications. Different biosensors, including immunosensors and DNA sensors, have been developed using functionalized magnetic nanoparticles for their operation in vitro and in vivo. Their use for magnetic targeting (drugs, genes, radiopharmaceuticals), magnetic

resonance imaging, diagnostics, immunoassays, RNA and DNA purification, gene cloning, cell separation, and purification has been developed. Moreover, magnetic nano-objects of complex topology, such as magnetic nano-rods and nanotubes, have been produced to serve as parts of various nano-devices, for example, tunable fluidic channels for tiny magnetic particles, data storage devices in nano-circuits, and scanning tips for magnetic force microscopes. [25]

Magnetic nanoparticles (MNPs) possess unique magnetic properties and the ability to function at the cellular and molecular level of biological interactions making them an attractive platform as contrast agents for magnetic resonance imaging (MRI) and as carriers for drug delivery. [26]

1.8 Properties of magnetic nanoparticles

Assessment of magnetic properties of nonmaterial is very important in estimating their stability, efficiency, separation, recovery and recyclability MNPs which exhibit permanent magnetization even after being removed from a magnetic field are referred to as ferromagnetic particles, whereas when paramagnetic particles are removed from a magnetic field, no permanent magnetization is observed. Magnetism or magnetic properties of NPs depend primarily upon two factors, magnetic induction, and strength of magnetic field. The magnetic properties also help in limiting the need to separate the catalyst by centrifugation, filtering, or extraction processes. [27]

1.9 Green Synthesis of Nanoparticles

Green synthesis of nanoparticles is the field of nanoparticle synthesis and assembly by utilization of biological systems such as yeast, fungi, bacteria and plant extracts. Generally, a lot of colloidal metal nanoparticles like platinum (PtNPs), gold (AuNPs), etc. [28] An array of new nanostructure components is burgeoning for various pharmaceutical and biomedical applications. The green chemistry method is the preferred approach for the synthesis of metal and metal oxide nanoparticles because of its low toxicity, environmental friendliness, feasibility, and safety to human health when compared with other chemical or physical methods. Plants are the most preferred source of all macro- and microscopic entities used for the green synthesis of nanoparticles due to the simplicity, non-toxicity, and easy availability of raw materials. Phytochemical such as flavonoids, alkaloids, steroids, phenolics, and saponins exhibit innate biological properties. Phytogenic synthesis of nanoparticles occurs at different physiochemical parameters. These parameters may help in controlling the shape, size, and disparity of

synthesised nanoparticles. Considering the importance of plant-mediated nonmaterial synthesis, in this chapter we provide a detailed account of the use of specific plant parts, different solvent media, key physiochemical parameters that direct the controlled synthesis of nanoparticles, and the mechanisms that mediate the nonmaterial synthesis. We also provide details on various specific phytochemical that act as reducing, capping, and stabilizing agents in the process of nanoparticle synthesis. [29]

1.10 Application of Nanoparticles

Nanotechnology is helping to considerably improve, even revolutionize, many technology and industry sectors: information technology, homeland security, medicine, transportation, energy, food safety, and environmental science, among many others.[30]

1.10.1 Biomedical application

Nanoparticles can be used for drug delivery, targeted drug delivery aims to deliver anticancer drugs specifically to the tumor site, minimizing damage to healthy cells. Chemotherapy, while effective, can have negative side effects by attacking healthy cells and organs. Magnetic nanoparticles coated with biocompatible materials like gold or polymers are used in targeted drug delivery. External magnetic field guides the drug/nanoparticle complex to the tumor site, where the drug is released through enzyme activity or changes in pH, temperature, or osmolality. Nanoparticles can be used as bioreceptors when coated with a bio responsive shell. Biosensors are used in various industries, including environmental, bio/pharmaceutical, and medical industries. [31]

1.10.2 Environmental application

Nanoparticles (NPs) have various applications in reducing soil pollution, such as in remediation processes and improving the efficiency of fertilizers, herbicides, pesticides, and growth promoters. This leads to lower doses, reduced side effects, pollutant release, and energy consumption. For example, Zn and Al NPs can be used for controlled release of nutrients, and mesoporous silica can protect pesticides from degradation. NPs are also useful in soil and water remediation, with materials like Zn and FeO NPs degrading dyes, drugs, and removing heavy metals. NPs can also be used for water decontamination, with carbon nanotubes and graphene oxide NPs having high adsorption capacity for organic pollutants and heavy metals. Metallic iron is effective in decontamination and water treatment for various compounds. Nanotechnology shows promise in the pursuit of clean and renewable energy sources. Solar photovoltaic energy, derived from sunlight, is efficient and versatile. However, challenges like high

production costs and low energy absorption efficiency remain. Carbon nanotubes offer an alternative material for cell structuring, with efficient energy capture and storage capabilities. TiO2 NPs have exceptional adsorption and photocatalytic activity, making them suitable for solar energy collection. [32]

1.10.3 Catalysis application

Currently, nanoparticles are increasingly substituting conventional heterogeneous catalysts. Due to smaller sizes, nanoparticles have higher surface area and increased exposed active sites. In that way nanoparticles have larger contact areas with reactants and are catalytically more active than conventional heterogeneous catalysts. Variations in shape and composition of nanocatalysts give access to different types of catalytic sites. A particular type of site displays better selectivity towards a particular reaction pathway. Thus, from the point of view of increased activity and selectivity nano catalysts have properties which tend to those of homogeneous catalysts. On the other hand, nano catalysts are relatively easier to separate from the reaction mixtures and therefore, in that sense, are heterogeneous catalysts. Furthermore, adsorption of reactant(s) on to the Nano catalyst is a necessary pre-condition for any nano-catalyzed reaction. This is again characteristic of a heterogeneous catalytic process. [33]

1.11 Photo Catalysis Adsorption of Nanoparticles

Photocatalysis utilizes radiation from UV to infrared, including visible light. It is a significant area of catalysis, especially for organic synthesis reactions. Photocatalytic reactions involve using light to degrade organic molecules, particularly dyes. Nanoparticles, like titanium dioxide, zinc oxide, and aluminum oxide, facilitate these reactions by forming oxygen-based radicals under visible or UV light. They can remove dyes, such as malachite green and methylene blue. These nanoparticles also aid in removing bacteria from surfaces, fuel photocatalytic reactions in solar cells, and degrade phenol-containing compounds in water systems.[34]

1.12 Literature Review

SELIMA, S and et al were synthesized a Nano-crystalline cupper ferrites ($CuFe_2O_4$) co-precipitation, solid-state reaction, thermal decomposition, sol-gel, and solution auto combustion methods. The samples were characterized by several techniques including XRD, FT-IR, SEM, TEM, and BET. Differences in crystallinity, surface area, particle size, magnetic parameters and catalytic properties of the prepared ferrite nanoparticles were observed. X-ray analysis showed that all samples, except sample prepared by auto combustion method (Cu_{aut}), are indexed as a cubic spinel structure with crystallite size lie in the range of 10–53 nm, whereas Cu_{aut} sample showed an amorphous structure. FT-IR spectra confirmed the formation of the $CuFe_2O_4$nanoparticles and displayed clear absorption peaks at ~ 600 and 400 cm−1 which are characteristic for cubic spinel crystal structure. Ferrite samples showed strong optical absorption in the visible region at 520–620 nm. The photoluminescence results explored emission peaks in the range of visible region at 405–425, 450–460, 520–530 and 570–590 nm. All samples exhibited a superparamagnetic behaviour, where the magnetic parameters are greatly changed by the preparation method and showed highest saturation magnetization of 29.04 emg/g for Cutherm sample and highest coercivity of 450 Oe for Cugel sample prepared by sol-gel method. The surface and textural properties of the produced samples were also found to depend on the synthetic process. All the prepared CuFe2O4 samples enhanced the thermal dissociation of ammonium perchlorate through a catalytic proton mechanism with the highest efficiency for Cugel sample.[35]

AMULYA, MA Shilpa. Were studied Morphological, electrochemical, and dye photodegradation on $CuFe_2O_4$ nanoparticles (NPs) prepared by a probe sonication method. Powder X-ray diffraction (PXRD) analysis indicated an average crystal size of 35–40 nm for the synthesized NPs. Diffuse-reflectance spectroscopy (DRS) and measurement of the band-gap energy indicated semiconductor behaviour. Vibrating sample magnetometry (VSM) studies at 300 K clearly revealed that $CuFe_2O_4$ NPs exhibit weak ferromagnetic behaviour. Electrochemical impedance spectroscopy (EIS) and cyclic voltammetry (CV) have been applied to analyse the electrochemical properties of the NPs. A $CuFe_2O_4$ NP electrode showed a greater response in an acidic medium (0.1 m HCl) than in a basic medium (0.1 m NaOH). Specific capacitance values of 1.54 and 0.02 F g^{-1} were calculated from cyclic voltammograms at the

$CuFe_2O_4$ electrode vs. an Ag/AgCl electrode in 0.1 m HCl and 0.1 m NaOH, respectively, at a scan rate of 10 mV/s. The electrode also showed high sensitivity for paracetamol, good cycling stability, and high-rate capability. From EIS data, the $CuFe_2O_4$ NPs showed pseudocapacitive characteristics. $CuFe_2O_4$ NPs have been employed as a photocatalyst for the removal of Methylene blue (MB) and Drimarene yellow (DY) dyes, whereby pH proved to be crucial. Under UV light, the degree of photocatalytic degradation was found to be high for MB (94%) but low for DY (29%).[36]

Harinee Subramanian a, and et al were used a one-step hydrothermal approach make pure magnetic copper ferrite ($CuFe_2O_4$) and copper ferrite-graphene oxide ($CuFe_2O_4$-rGO) nanocomposites (NCs) and spinel structure $CuFe_2O_4$ with a single phase of tetragonal $CuFe_2O_4$-rGO-NCs was confirmed by the XRD. Then, characterization of $CuFe_2O_4$-rGO-NCs was done using ng Raman spectroscopy, FT-IR, TGA-DTA, EDS, SEM, and TEM. The synthesized NCs was exposed to UV light to evaluate its photocatalytic activity for the degradation of methylene blue (MB) and rhodamine B (RhB) with $CuFe_2O_4$and $CuFe_2O_4$-rGO-NCs, respectively. The catalyst $CuFe_2O_4$-rGO-NCs provided higher degradation of MB (94%) than for RhB (86%) under UV light irradiation compared to $CuFe_2O_4$. Further, the antibacterial activities of $CuFe_2O_4$-NPs and $CuFe_2O_4$-rGO-NCs were tested against Gram-negative and -positive bacterial pathogens such as Vibrio cholera (V. cholera); Escherichia coli (E. coli); Pseudomonas aeruginosa (P. aeruginosa); Bacillus subtilis (B. subtilis); Staphylococcus aureus (S. aureus); and Staphylococcus epidermidis (S. epidermidis) by well diffusion method. At 100 μg/mL concentrations of $CuFe_2O_4$-rGO-NCs, maximal growth inhibition was shown against E. coli (18 mm) and minimum growth inhibition against S. epidermidis (12 mm). This study suggests that $CuFe_2O_4$-rGO-NCs as a high-efficacy antibacterial material and plays an important role in exhibiting higher sensitivity depending on concentrations. The results encourage that the synthesized $CuFe_2O_4$-rGO-NCs can be used as a promising material for the antibacterial activity and also for dye degradation in the water/wastewater treatment plants.[37]

Harinee P. , and et al recognized copper ferrite nanoparticles, for their ferromagnetic characteristics, minimal conductivity, and superior electrochemical stability, were synthesized by a facile auto combustion approach using egg white as fuel via a green synthesis route. $CuFe_2O_4$ nanoparticles' structural, morphological, and optical

properties were examined. XRD is used to determine the phase formation, particle size, and lattice parameter of spinel ferrite. X-ray Diffractometer (XRD), Fourier Transform Infrared Spectrometer (FTIR), Scanning Electron Microscopy (SEM), and Energy Dispersive X-ray analysis were used to rigorously examine the phase purity of the synthesized spinel ferrite. For morphological analysis, SEM and TEM were employed, whereas EDAX was used for elemental analyses. For a better knowledge of the conduction band (CB) and valence band (VB) boundaries of the produced nanoparticles, optical experiments were conducted by UV Diffuse Reflectance Spectroscopy. The degradation of Rhodamine B dye determined the photocatalytic competence of the synthesized sample under visible light. At regular intervals of time, the entire process was observed with a spectrophotometer. $CuFe_2O_4$ nanoparticles reveal a maximum photocatalytic degradation efficiency of around 94%, which is higher than that of $CuFe_2O_4$ nanoparticles prepared via another chemical route.[38]

Saade A. and et al were eco-friendly synthesized magnetic spinel copper ferrite ($CuFe_2O_4$) nanostructures using Nasturtium officinale extract. Physicochemical properties of these nanostructures were determined by transmission electron microscopy, field emission scanning electron microscopy (FE-SEM), X-ray diffraction (XRD), vibrating sample magnetometry, and energy dispersive X-ray mapping analysis. XRD patterns conform to the $CuFe_2O_4$formation. SEM results demonstrated ceramic spinel CuFe2O4 nanostructures with spherical surface morphologies. The cytotoxicity effect of $CuFe_2O_4$ nanostructures against rat pheochromocytoma (PC12) cells was evaluated based on MTT assay. The magnetic nanostructures had low toxicity at a concentration of 250 µg/mL. It appears that these nanostructures can be considered as suitable candidates for drug delivery and other biomedical applications, because of their low toxicity effects.[39]

Anukorn P. and et al were prepared Copper ferrite ($CuFe_2O_4$) nanoparticles in alkaline solutions containing Cu $(NO_3)_2 \cdot 6H_2O$ and $Fe(NO_3)_3 \cdot 9H_2O$ with the pH of 6–12 by microwave-hydrothermal method. The as-prepared products characterized by XRD were specified as cubic $CuFe_2O_4$phase. Average sizes of the $CuFe_2O_4$ nanoparticles calculated by Scherrer formula are in the same range as those obtained by TEM analysis. FTIR shows main transmittance band at 585 cm^{-1}, corresponding to stretching mode of tetrahedral complexes. Saturation magnetization, remanence and coercivity

were increased with increasing in the particle-size and crystalline degree of the nanoparticles.[40]

Zhipeng S. and et al were synthesized Semiconductive nanometer-size material $CuFe_2O_4$ by a low-heating solid-state reaction of inorganic reagents of Cu $(CH_3COO)_2 \cdot H_2O$, Fe $(NO_3)_3 \cdot 9H_2O$ and NaOH. The process was a convenient, environment friendly, inexpensive and efficient preparation method for the $CuFe_2O_4$ nanomaterial. X-ray diffraction (XRD) was used to confirm the material structure and scanning electron microscopy (SEM) to depict the crystallite microstructure. Conductance responses of the nanocrystalline $CuFe_2O_4$ thick film were measured by exposing the film to reducing gases of ammonia (NH_3), acetone (CH_3COCH_3), hydrogen (H_2) and ethanol gas (C_2H_5OH). It was found that the sensor exhibited various sensing responses to these gases at different operating temperatures. Furthermore, the sensor exhibited a fast response and a good recovery.[41]

1.13 Aim of the work

- Green synthesis of copper ferrite nanoparticles using Foeniculum vulgare extract.
- Characterization of copper ferrite nanoparticles using Scanning electron microscopy (SEM), Energy Dispersive X-Ray (EDX), Fourier transform infrared (FTIR), X-Ray diffraction (XRD), and surface area (BET)).
- Adsorption and photocatalysis study.

Chapter 2

Experimental Part

2.1 Materials

- Fennel seeds
- $Cu(NO_3)_2.3H_2O$
- $Fe(NO_3)_3.9H_2O$

2.2 Method

2.2.1 Preparation of Fennel Seeds Extract

10g of Fennel seeds was placed in 100 ml distilled water and the mixture was boiled under the stirring for 20 min., then the yellow color solution was obtained. The extract was cooled at room temperature and filtered.

2.2.2 Synthesis of $CuFe_2O_4$NPs

$CuFe_2O_4$ were bio generated by Fennel seeds extract. 12.1g of $Cu(NO_3)_2.3H_2O$ and 40.4g of $Fe(NO_3)_3.9H_2O$. Each substance was placed in a beaker containing 100 ml of distilled water, stirring until all the substances were dissolved. After the solution were prepared, they were mixed together and stirred for 30 min. 30 ml of Fennel seed solution was added while continuing to stir on the hot plate until the thick gel formed. The formed gel was placed in the oven at 150 ^{0}C until it dries completely, then was grinded to converted into powdered form. The obtained powder was placed in a furnace for 5 hours at 700 C to eliminate the impurities to obtain the $CuFe_2O_4$ – NPs.

2.2.3 Adsorption Studies

All adsorption investigations were conducted with Malachite Green (MG) as the reference dye. MG is basically a cationic dye classed as a triarylmethane chloride dye. $C_{23}H_{25}ClN_2$ has a molar mass of 365. The intense blue color of the dye is due to its strong absorption in visible region at 618 nm.

MG dye was prepared by dissolving 10mg in 1L of distilled water. The concentration of malachite green was determined to be 10 ppm, from which various aliquots of the experimental sample were obtained. After each experiment, the concentration of MG was evaluated by measuring the absorbance in the visible area with a UV–Vis absorption spectrophotometer. To prevent photolysis, batch adsorption operations were conducted in foil-lined glass beakers using a magnetic stirrer at room temperature.

The quantity of MG absorbed per gram of nanoparticles at time (min) can be calculated by the following Eq (1).

$$\mathrm{qt} = (C_0 - C_t)\frac{\mathrm{V}}{\mathrm{m}}$$

Where C_0 and C_t are the initial and equilibrium concentrations of the dye, V is the dye solution volume, and m is the adsorbent's mass.

2.2.4 Photo-catalytic Activity

In aqueous solution, synthesized materials were employed to photo catalytically adsorb MG dye as a model of dye pollution. 100 milligrams of $CuFe_2O_4$ were added to the MG dye solution (100 mL of 10ppm). In the beginning, the suspension was vigorously swirled in the dark for four hours to ensure complete dye adsorption on the catalyst. Additionally, the suspension was illuminated with visible light. After every 10 minutes (three times), then 30 minutes, 4 mL of dye solution was removed and filtered using micro filter. Using a UV–Vis spectrophotometer, the absorbance of a solution was evaluated. The percentage of dye got adsorbed for different adsorbent loading is calculated using the Eq. (2).

$$\%\text{Adsorption} = \frac{C_0 - C_t}{C_0} \times 100$$

where C_0 is the starting concentration of dye and Ct is the concentration of dye following adsorption by copper ferrite nanoparticles after t seconds.

2.2.5 Effect of Adsorbent Mass

To investigate the effect of adsorbent mass, different masses of adsorbent 25, 50, 75, 100 and 125mg were introduced in several beakers containing a specific volume of a fixed MG dye (100ml), at the same pH and room temperature. The concentration of MG was measured at equilibrium.

2.2.6 Effect of pH on the adsorption of MG dye

To investigate the effect of pH, several beakers containing 50ml of MG dye were rendered to pH 2, 4, 6, 8 and 10. After which, 100mg of copper ferrite were introduced in all beakers at room temperature. The concentration of MG was measured at equilibrium.

2.3 Characterization of $CuFe_2O_4$ NPs

$CuFe_2O_4$ nanoparticles obtained was characterized using x-ray diffraction (XRD), energy dispersive x-ray (EDX), scanning electron microscopy (SEM) UV– Visible spectrometer, Brunauer Emmett Teller analyzer (BET) and Fourier transform infrared spectroscopy (FT-IR). The furnace was used for calcination purposes, the phase structure and average crystallite size of the nanoparticles were investigated by examining the powder's XRD patterns. The structural morphology and chemical

composition of $CuFe_2O_4$ nanoparticles were examined and measured by SEM – EDX. The samples were previously oven-dried at 105 °C. The mode of chemical bonding in the samples was studied by FTIR in the range of 4000–400 cm^{-1}.The samples' porosity was determined using N_2 adsorption-desorption isotherms at the N_2 boiling point (77 K). Before the adsorption experiment, the specimen was degassed with He for two hours at 250 °C to remove moisture and adsorbed contaminants. The BET (Brunauer, Emmett and Teller) formula and the t-plot method of Lippens and de Boer were used to estimate the porosity and surface area.

Chapter 3

Results and Discussion

3.1 Scanning Electron Microscopy (SEM)

The scanning electron microscope (SEM) is a powerful tool for taking very high magnification images of a variety of materials. SEM images for surface morphology of $CuFe_2O_4$ nanocomposites are shown in Figure (1). It can be observed that there are spherical shaped particles with different sizes throughout a range of 30.8-43.6 nm.

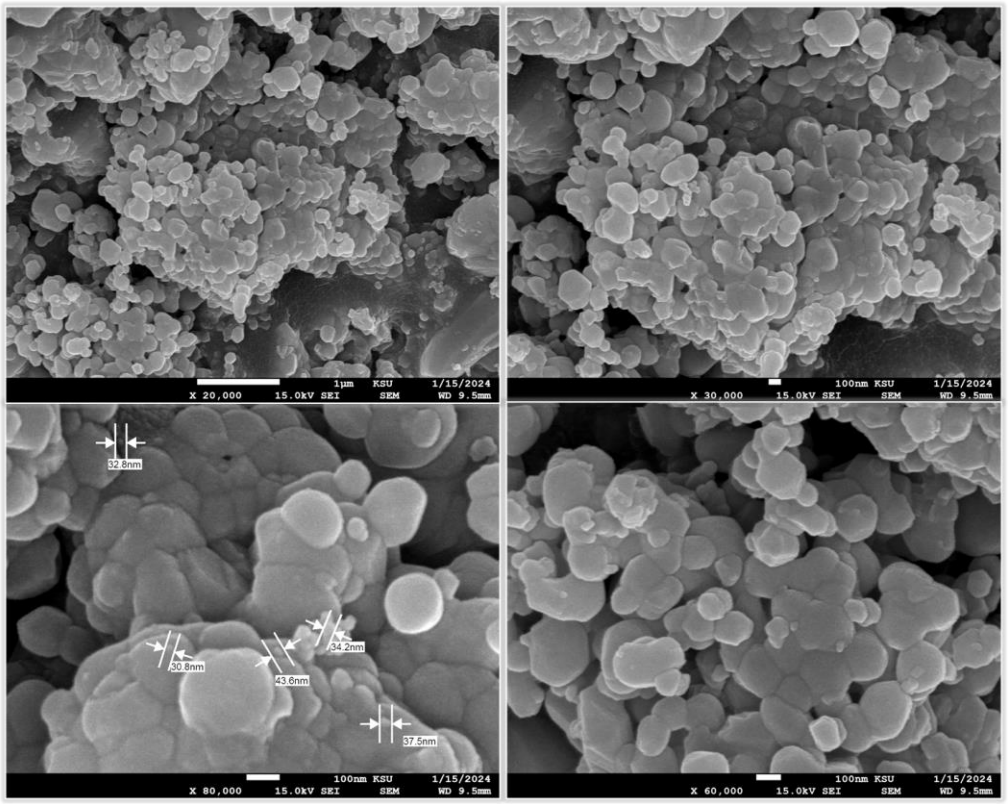

Figure (1): SEM image of $CuFe_2O_4$NPs at different magnifications

3.2 Energy-Dispersive X-Ray Spectroscopy (EDX)

EDX is one of the powerful tools for describing the percentage of elemental composition in the sample which is shown in Figure (2). EDX analysis was performed on $CuFe_2O_4$ nanocomposites. The results showed the presence of iron (Fe), Copper (Cu), and oxygen (O) elements in the $CuFe_2O_4$ nanocomposites with weight percent equal to 40.3%, 27% and 32.7% respectively. No other impurity components are present in the samples, so that the prepared samples are defect-free and homogenous.

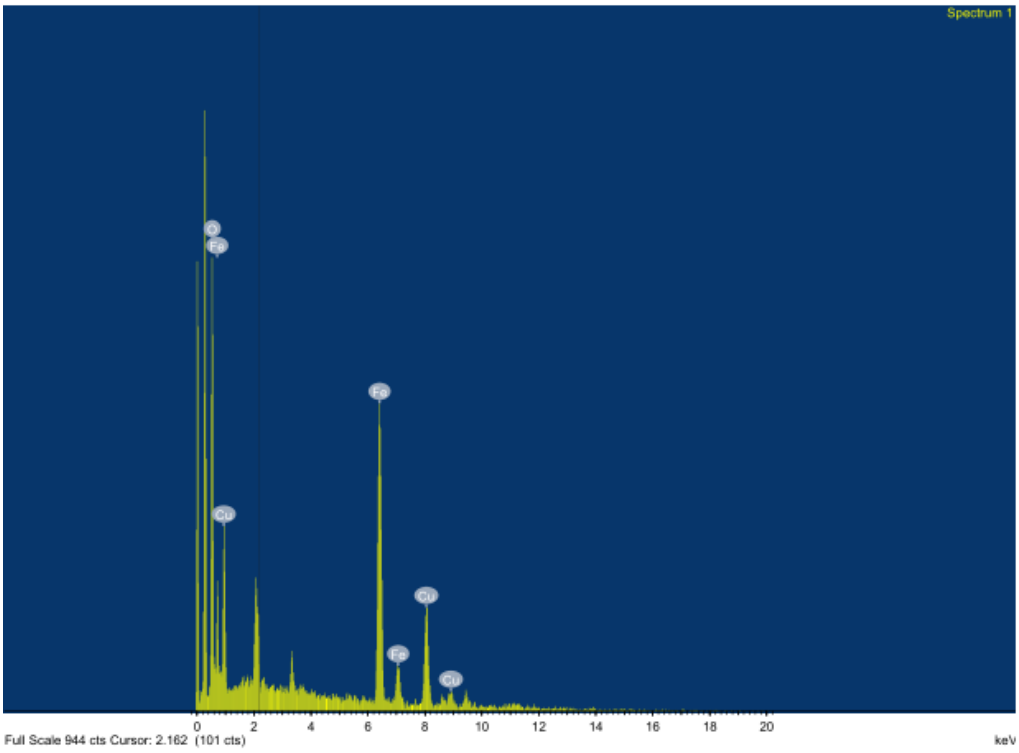

Figure (2): EDX analysis of $CuFe_2O_4$ Nanoparticles

3.3 Infrared Spectroscopy (IR)

Figure (3) shows the FT-IR spectrum of the $CuFe_2O_4$ in the wave-number range between 400 and 4000 cm^{-1}. At 3440 cm^{-1} there is a broadband of OH group that indicates presence of moisture on the surface of $CuFe_2O_4$ nanocomposite. The absorption bands at 415.55, 579.02 and 589.77 cm^{-1} are caused by the stretching vibrations of Cu–O and Fe–O bonds inside copper ferrite nanoparticles. Two weaker bands appear at 1343 and 1633 cm^{-1} are ascribed to the surface of hydroxyl bending that were adsorbed on the surface of $CuFe_2O_4$ NPs.

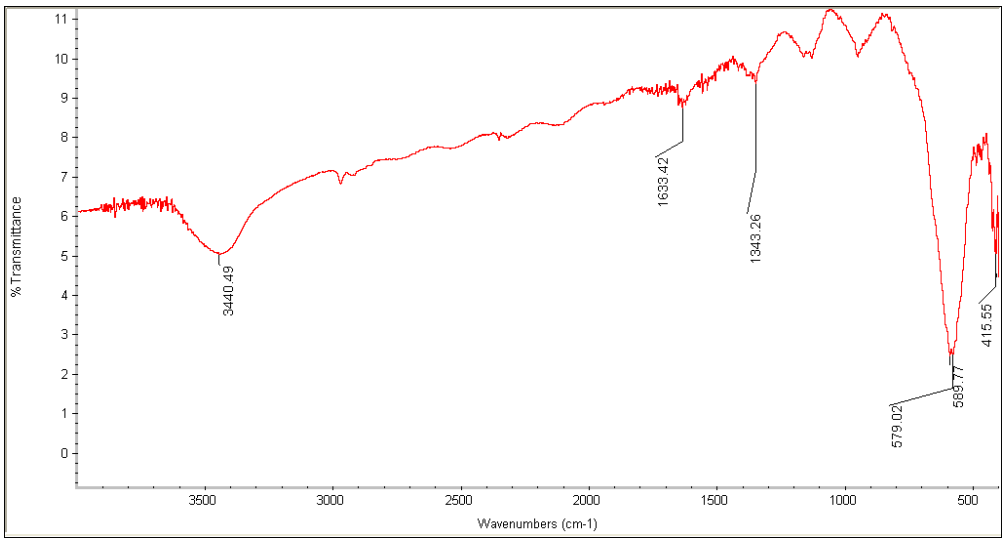

Figure (3): IR Spectrum of $CuFe_2O_4$ Nanocomposites

3.4 X-Ray Diffraction (XRD)

Figure (4) depicts the X-ray diffraction pattern of $CuFe_2O_4$ nanoparticles. Synthesized $CuFe_2O_4$ nanoparticles exhibited diffraction peaks with 2θ values corresponding to planes (111), (220), (311), (222), (400), (422), (511), (440) and (533). This confirmed the cubic structure of $CuFe_2O_4$ nanoparticles according to JCPDS card number 82-1042. The sample's phase purity is ensured by the absence of impurity peaks.

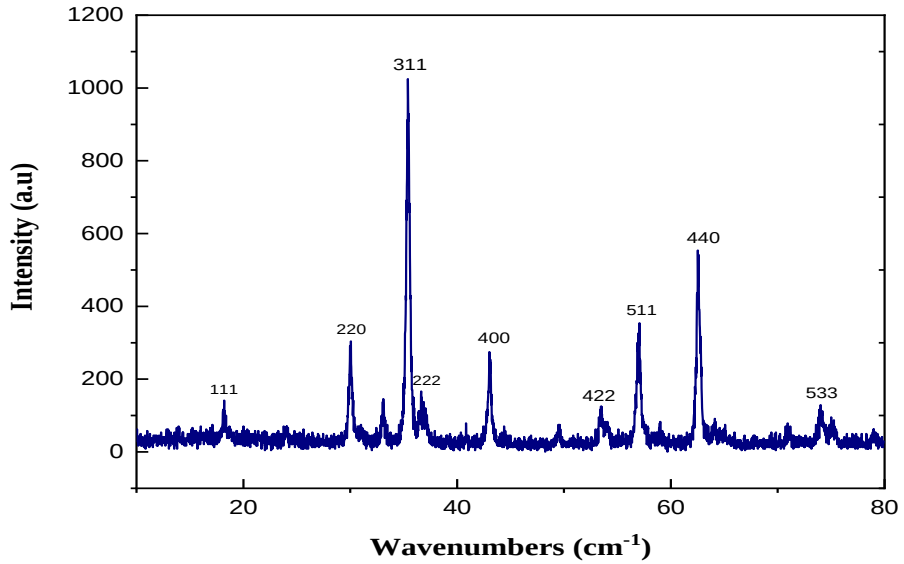

Figure (4): XRD Patterns for $CuFe_2O_4$ Nanoparticles

3.5 The Surface Area (BET)

The identification of nanoparticles relies heavily on the measurement of their specific surface area. In the case of $CuFe_2O_4$ NPs, their surface area was assessed through the use of the BET and BJH methods. Nitrogen is commonly utilized in BET analyses due to its exceptional purity and strong affinity for most solids. The process involves the adsorption of Nitrogen onto the surface of $CuFe_2O_4$ NPs at a constant temperature, providing valuable insights into their characteristics. It is confirmed that the nanoparticles have spherical-shaped pores and exhibit a type H3 hysteresis loop, as shown in (Figure 5a). This indicates the mesoporous nature of the particles. The results indicate that $CuFe_2O_4$ NPs have a surface area of 20.35 m^2/g, which is a considerable value. In addition, the pore volume and pore size are 0.092 cm^3/g and 161.230 Å, respectively. The isotherm observed from the N_2 sorption indicates that it belongs to the Langmuir type IV, as shown in (Figure 5b). The mesoporous materials were characterized by their BET surface area. At the lower pressure regions, it shows the formation of a monolayer followed by a formation of multilayers, with a relative pressure (P/Po = 0.02-0.99).

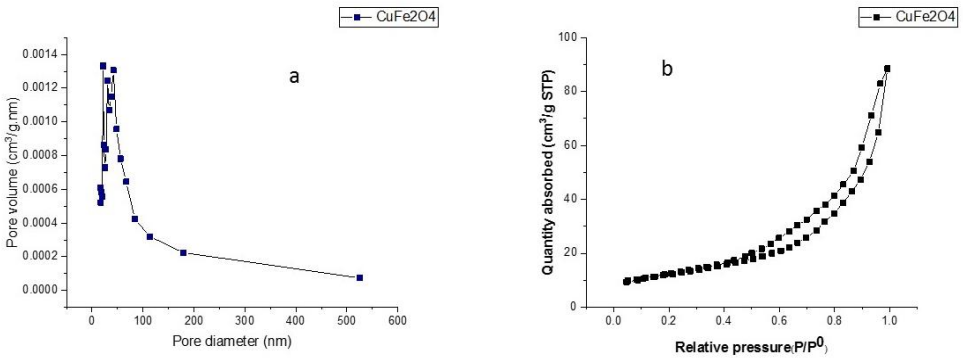

Figure (5): (a) (BJH) pore size distribution and (b) N_2 adsorption – desorption isotherm (BET) $CuFe_2O_4$

3.6 Adsorption Study and Contact Time

$CuFe_2O_4$ nanocomposite served as an adsorbent to evaluate MG adsorption. Equilibrium contact time is one of most significant parameters affecting the design of contaminated water treatment system. The effect of equilibrium time on MG dye adsorption was shown in Figure (6). A note can be made that is that the adsorption increases rapidly at first then the process of adsorption slows down as it gradually approaches an equilibrium. The contact time and equilibrium adsorption capacity q_e were about 240 min and 17.71mg/g in the MG dye of 10 ppm.

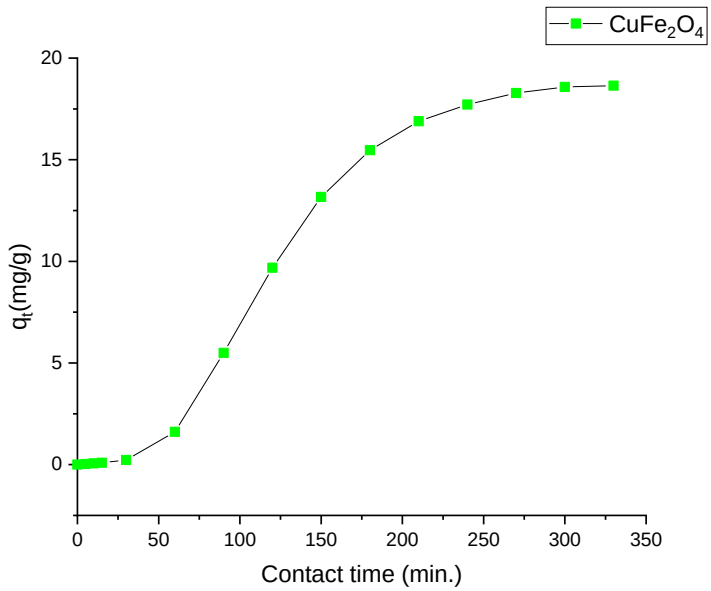

Figure (6): Adsorption Capacity of $CuFe_2O_4$ at Different Contact Time

3.7 Photocatalytic Degradation

The photocatalytic properties of the prepared $CuFe_2O_4$ nanocomposite were evaluated via adsorption of MG dye in aqueous solution under visible illumination source. The rate of decomposition process of dye was measured by observing the characteristic absorption peak at 618 nm and measuring the gradual reduction in concentration at different time intervals. The obtained results show higher photocatalytic degradation of MG under visible radiation. The removal percentage of MG was 99%. These results make copper ferrite nanocomposite an excellent catalyst for degradation of MG dye pollutant.

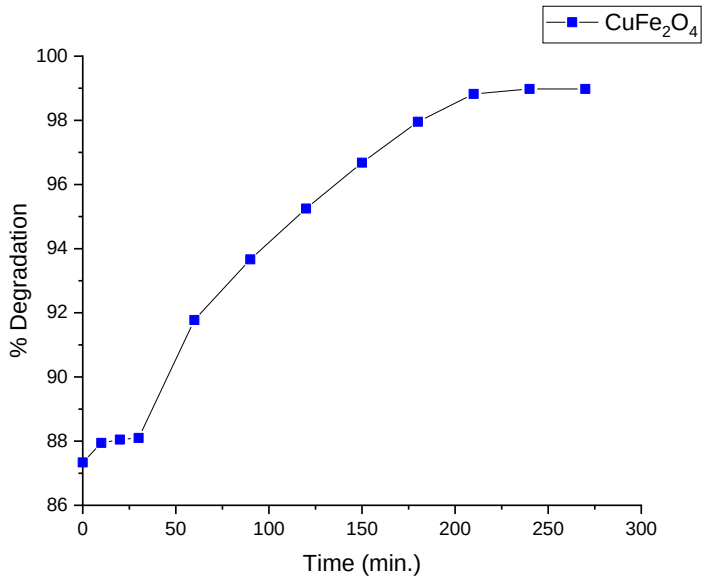

Figure (7): Photocatalysis Percentage Efficiency

3.8 Effect of Adsorbent Mass

Adsorbent mass is another factor that can affect adsorption. It demonstrated the relation between the mass of $CuFe_2O_4$ nanocomposite and the adsorption of MG dye. In general, it was found that the percentage of adsorbed MG dye increased as the mass of $CuFe_2O_4$ increased. This can be interpreted by the increase in adsorption sites that resulted from increasing the mass of adsorbent nanocomposite to interact with MG molecules.

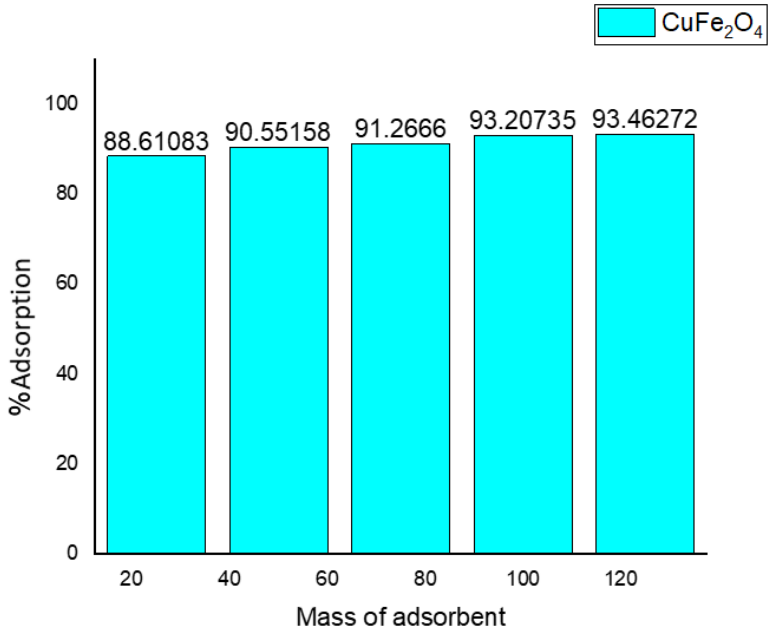

Figure (8): Effect of different Adsorbent Doses on Adsorption Process

3.9 Effect of Adsorbent pH

The pH effect on the adsorption of MG by $CuFe_2O_4$ NPs was studied at pH values ranged from 2.0 to 10.0. The results were showed in Figure 9. The adsorption of dye by $CuFe_2O_4$ NPs reached its maximum at pH 8. However, the adsorption percentage decreased by increasing pH above 8.0. In addition, these results are somewhat expected since an alkaline medium may convert these dyes to their salt forms and thus and thus the electrostatic repulsion between the negatively charged MG and $CuFe_2O_4$ sites.

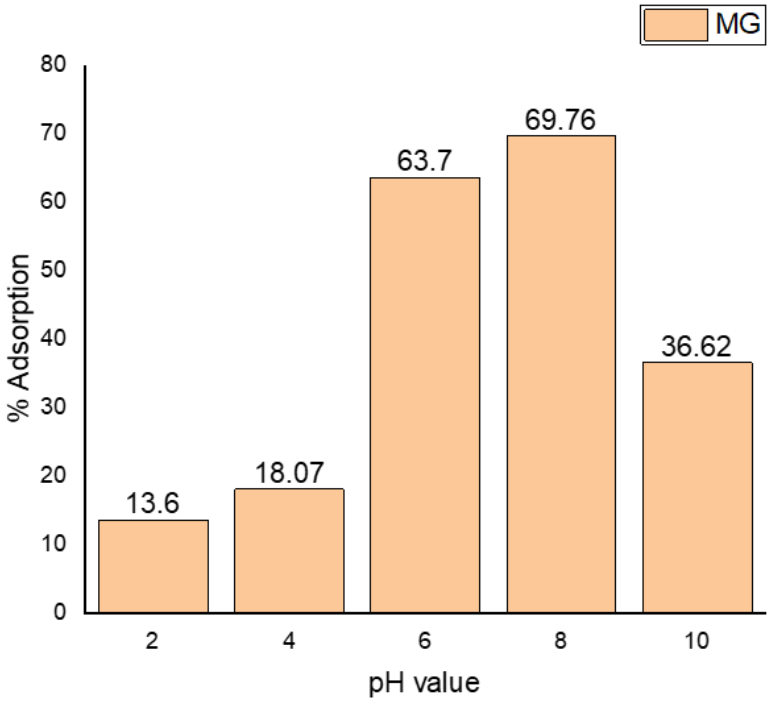

Figure (9): The pH Effect on the adsorption of MG by $CuFe_2O_4$ nanocomposite

Chapter 4
Conclusion and Recommendation

4.1 Conclusion

Throughout this study, we have been successfully synthesizing Copper ferrite nanocomposite by using the precipitation method. The approach used for the synthesis was simple, low cost, rapid, nontoxic, and eco-friendly. $CuFe_2O_4$ nanoparticles were synthesized through the reaction of $Cu(NO_3)_2$ and $Fe(NO_3)_2$ and non-toxic Foeniculum vulgare seeds extract. The obtained $CuFe_2O_4$ NPs were characterized by SEM, EDX, FITR, XRD, and BET. SEM images for surface morphology of $CuFe_2O_4$ nanocomposites observed there are spherical shaped particles with different sizes. The results of EDX analysis indicated the high purity of the synthesized sample. The appearance of some functional groups was confirmed by FTIR analysis. XRD was used to evaluate the peak intensity, position, and width of the nanoparticles, which confirms the purity and formation of nanocomposite. The pore size distribution and N_2 adsorption –desorption isotherm was confirmed by BET analysis of copper ferrite nanoparticles. The findings demonstrated that the adsorption time was reaching equilibrium within 240 min and adsorption capacity of 17.71 mg. g^{-1}. The photocatalytic degradation of MG dye was investigated and $CuFe_2O_4$ nanocomposite was exhibited superior photocatalyst. Furthermore, the fabricated photocatalyst $CuFe_2O_4$ is proposed to be magnificent candidates as photocatalyst for organic pollutants in industrial wastewater.

4.2 Recommendation

- Characterization of $CuFe_2O_4$ -NPs via TEM analysis.
- Study of the magnetic and optical properties of $CuFe_2O_4$ -NPs.
- Evaluation of Copper ferrite NPs effectiveness in batteries.
- Examination of antimicrobial activity /sanitizing ability of $CuFe_2O_4$-NPs.
- Exploration of $CuFe_2O_4$ -NPs sensing ability of gases or biomolecules and investigation of sensing mechanism and its relation to conductivity.

References:

1. SILVA, Gabriel A. Introduction to nanotechnology and its applications to medicine. *Surgical neurology*, **2004**, 61.3: 216-220.
2. THOMAS, Sabu, et al. *Foundations of nanotechnology, volume two: nanoelements formation and interaction*. CRC Press, **2014**.
3. KELSALL, Robert W.; HAMLEY, Ian W.; GEOGHEGAN, Mark. *Nanoscale Science and Technology*. **2005**.
4. HONG, Nguyen Hoa. Nano-sized Multifunctional Materials: Synthesis, Properties and Applications. *Elsevier*, **2018**.
5. Green Synthesis of Nanomaterials for Bioenergy Applications UK: *Wiley*, **2020**.
6. KUMAR, Vineet, et al. Functionalized Nanomaterials. CRC Press, 2021.
7. SINGH, Veer; YADAV, Priyanka; MISHRA, Vishal. Recent advances on classification, properties, synthesis, and characterization of nanomaterials. *Green synthesis of nanomaterials for bioenergy applications*, **2020**, 83-97.
8. SANNINO, Diana. Types and classification of nanomaterials. *Nanotechnology: Trends and Future Applications*, **2021**, 15-38.
9. Okuyama, K., Lenggoro, W., & Iwaki, T. Nanoparticle preparation and its application: A nanotechnology particle project in Japan. In Proceedings of the 2004 International Conference on MEMS, NANO and Smart Systems. *IEEE*. pp. 1-4. **2004**
10. Akbarzadeh, A., Samiei, M., & Davaran, S. Magnetic nanoparticles: preparation, physical properties, and applications in biomedicine. *Nanoscale Research Letters*, **2012**. 7(1), 1441.
11. Fabian FA, Pedra PP, Duque JG, Meneses CT. Synthesis and characterization of La (Cr, Fe, Mn) O_3 nanoparticles obtained by co-precipitation method. *Journal of Magnetism and Magnetic Materials*. **2015**. 1;379:80-3.
12. Bajaj, N.S., and R.A. Joshi. "Energy Materials: Synthesis and Characterization Techniques. *Energy Materials*, **2020**, pp. 61-82
13. Hasnidawani, J.N., et al. Synthesis of ZnO Nanostructures Using Sol-Gel Method. *Procedia Chemistry*, **2015**. 19. 211-216.
14. CATAURO, M. et al. The Influence of the Polymer Amount on the Biological Synthesized Properties via Sol-Gel of PCL/ZrO Technique 2 Hybrid Materials. *Sol-Gel Chemistry Applied to Materials Science*, **2019**, 14.

15. Bokov, D., Turki Jalil, A., Chupradit, S., Suksatan, W., Javed Ansari, M., Shewael, I. H., ... & Kianfar, E. Nanomaterial by sol-gel method: synthesis and application. *Advances in Materials Science and Engineering*, **2021**, 2021: 1-21.
16. Jain, R, Chaurasia, SK., Kalga, A; Report on Sol gel method for nanoparticle synthesis, **2012.**

    Rane, A. V., Kanny, K., Abitha, V. K., & Thomas, S. Methods for synthesis of nanoparticles and fabrication of nanocomposites. In: *Synthesis of inorganic nanomaterials*. *Woodhead Publishing*, **2018**, 121-139.
17. Sivakumar, M., Kannan, S., Tiwari, A. K., Mishra, J. N. Lee, & A. P. Advanced materials for agriculture, food, and environmental safety. **2013**.
18. Titus, D., Samuel, E. J. J., & Roopan, S. M. Nanoparticle characterization techniques. In Green synthesis, characterization and applications of nanoparticles. *Elsevier*. **2019**, 303-319.
19. PAL, Sovan Lal, et al. Nanoparticle: An overview of preparation and characterization. *Journal of applied pharmaceutical science*, **2011**, 228-234.
20. Hwang, N., & Barron, A. R. BET surface area analysis of nanoparticles. *The connexions project*. **2011**, 1-11.
21. Holder, C. F., & Schaak, R. E. Tutorial on powder X-ray diffraction for characterizing nanoscale materials. *Acs Nano*. **2019**. *13*(7), 7359-7365.
22. DUTTA, Aastha. Fourier transform infrared spectroscopy. Spectroscopic methods for nanomaterials characterization. *Elsevier,* **2017**, 73-93.
23. DYKSTRA, Michael J., et al. Specimen preparation for electron microscopy. Biological Electron Microscopy: Theory, Techniques, and Troubleshooting. *Springer*, **2003**, 1-73.
24. KATZ, Evgeny. Magnetic nanoparticles. *Magnetochemistry*, **2020**, 6.1: 6.
25. SCHLADT, Thomas D., et al. Synthesis and bio-functionalization of magnetic nanoparticles for medical diagnosis and treatment. *Dalton Transactions*, **2011**, 40.24: 6315-6343.
26. ALONSO, J., et al. Magnetic nanoparticles, synthesis, properties, and applications. In: Magnetic nanostructure materials. *Elsevier*, **2018**. 1-40.
27. ROY, Nidhija, et al. Green synthesis of silver nanoparticles: an approach to overcome toxicity. *Environmental toxicology and pharmacology*, **2013**, 36.3: 807-812.

28. THUNUGUNTA, Tejaswi; REDDY, Anand C.; REDDY DC, Lakshmana. Green synthesis of nanoparticles: current prospectus. *Nanotechnology Reviews*, *2015*, 4.4: 303-323.
29. Stark, W. J., Stoessel, P. R., Wohlleben, W., & Hafner, A. J. C. S. R. Industrial applications of nanoparticles. *Chemical Society Reviews.* **2015**, *44*(16), 5793-5805.
30. McNamara, K., & Tofail, S. A. Nanoparticles in biomedical applications. *Advances in Physics.* **2017**, *2*(1), 54-88.
31. Martínez, G., Merinero, M., Pérez-Aranda, M., Pérez-Soriano, E. M., Ortiz, T., Villamor, E., ... & Alcudia, A. Environmental impact of nanoparticles' application as an emerging technology: A review. *Materials***. 2020**, *14*(1), 166.
32. Astruc, D. (Ed.). Nanoparticles and catalysis. Hoboken, New Jersey, USA: *John Wiley & Sons*. **2008**.
33. Dave P. N. et al. Applications of nano-catalyst in a new era. *Journal of Saudi Chemical Society*, **2012**.
34. SELIMA, S. S.; KHAIRY, M.; MOUSA, M. A. Comparative studies on the impact of synthesis methods on structural, optical, magnetic and catalytic properties of $CuFe_2O_4$. *Ceramics International*. **2019**, 45.5: 6535-6540.
35. AMULYA, MA Shilpa, et al. Evaluation of bifunctional applications of $CuFe_2O_4$ nanoparticles synthesized by a sonochemical method. *Journal of Physics and Chemistry of Solids*, **2021**, 148: 109756.
36. SUBRAMANIAN, Harinee, et al. Hydrothermal synthesis of spindle structure copper ferrite-graphene oxide nanocomposites for enhanced photocatalytic dye degradation and in-vitro antibacterial activity. *Environmental Research*, **2023**, 231: 116095.
37. UDHAYA, P. Aji, et al. Copper Ferrite nanoparticles synthesised using a novel green synthesis route: Structural development and photocatalytic activity. *Journal of Molecular Structure*, **2023**, 1277: 134807.
38. JASIM, S. A., Patra, I., Opulencia, M. J. C., Hachem, K., Parra, R. M. R., Ansari, M. J., ... & Akhavan-Sigari, R. Green synthesis of spinel copper ferrite (CuFe2O4) nanoparticles and their toxicity. *Nanotechnology Reviews*. **2020**, *11*(1), 2483-2492.
39. PHURUANGRAT, A., Kuntalue, B., Thongtem, S., & Thongtem, T. Synthesis of cubic CuFe2O4 nanoparticles by microwave-hydrothermal method and their magnetic properties. *Materials Letters*. **2016**, 167, 65-68.
40. SUN, Z., Liu, L., zeng Jia, D., & Pan, W. Simple synthesis of $CuFe_2O_4$ nanoparticles as gas-sensing materials. *Sensors and Actuators B: Chemical*. **2007**, 125(1), 144-148.

Curriculum Vitae

Name: Anwar Aftan AlDhahi

ID: 440028553

Department: Chemistry.

University: Imam Muhammad Ibn Saud University.

E-mail: anwarrawna999@gmail.com

Name: Fay Shaya Al-Qahtani.

ID: 441018274

Department: Chemistry.

University: Imam Muhammad Ibn Saud University.

E-mail: fq76.al@gmail.com

Name: Lina Hajjaj Alhajjaj

ID: 441018810

Department: Chemistry.

University: Imam Muhammad Ibn Saud University.

E-mail: lina.alhajjaj@gmail.com

Name: Hala Mubarak Almouh

ID: 440027199

Department: Chemistry.

University: Imam Muhammad Ibn Saud University.

E-mail: halamm2000@gmail.com

Name: Haifa Mohammed Bin-Owais

ID: 441020300

Department: Chemistry.

University: Imam Muhammad Ibn Saud University.

E-mail: HaifaBinAwis@gamil.com